ACS OMEGA

Article

Cite This: ACS Omega 2018, 3, 6779−6786

Photobactericidal Activity of Dual Dyes Encapsulated in Silicone Enhanced by Silver Nanoparticles

Adnan Patir,[†] Gi Byoung Hwang,[†] Sean P. Nair,[‡] Elaine Allan,[‡] and Ivan P. Parkin*[,†]

[†]Materials Chemistry Research Centre, Department of Chemistry, University College London, 20 Gordon Street, London WC1H 0AJ, United Kingdom

[‡]Department of Microbial Diseases, UCL Eastman Dental Institute, University College London, 256 Gray's Inn Road, London WC1X 8LD, United Kingdom

Supporting Information

ABSTRACT: Crystal violet (CV) and methylene blue (MB) dyes with silver (Ag) nanoparticles (NPs) were encapsulated into silicone to produce light-activated antimicrobial surfaces. Optical microscopy and X-ray photoelectron spectroscopy showed that CV and MB were diffused throughout the silicone samples and that Ag NPs were successfully encapsulated by the swell−encapsulation−shrink process. Antimicrobial tests on *Staphylococcus aureus* and *Escherichia coli* showed that CV/MB-encapsulated silicone samples have stronger photobactericidal activity than CV or MB samples and the addition of Ag NPs significantly enhanced the antimicrobial activity under white light. The number of viable bacteria decreased below the detection limit (below $<10^3$ CFU) on the silicone-incorporating CV/MB/Ag NPs within 3 h for *S. aureus* and within 5 h for *E. coli*. In leaching tests over 216 h, the amount of dye leaching from the samples was barely detectable (<0.02 ppm). These surfaces have a potential for use in healthcare settings to decrease hospital-associated infections.

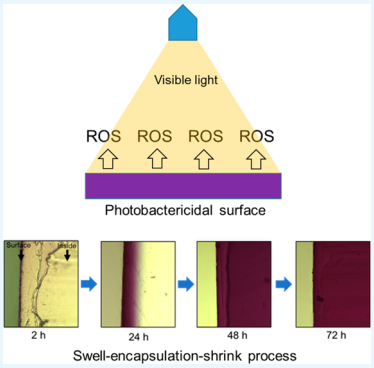

INTRODUCTION

The incidence of hospital-associated infections (HAIs) has been noted as "unacceptably high" by the National Institute for Health and Care Excellence. In the U.K., about 300 000 patients per year are treated for a HAI, such as surgical site infections (15.7%), infections of the urinary tract (17.2%), and lower respiratory tract or pneumonia infections (22.8%), at a cost of approximately £1 billion to the NHS[1−4] It is estimated that 1 of 16 patients who receive treatment in an NHS hospital in the U.K. would get a HAI.[2−4] Despite extensive effort, little has been accomplished to reduce the prevalence of hospital pathogens and hospitalized patients are still under risk due to the prevalence of HAIs.[2] The approximate cost of HAIs to U.S. hospitals was approximately U.S. $45 billion for hospital services related to inpatients and around 75 000 patients with HAIs died in 2011 according to the report by The Centers for Disease Control and Prevention.[5]

Most of the patients, visitors, and staff in hospitals do not apply the highest standards of personal hygiene, and almost 80% of nosocomial infections are transferred through touches between hospital surfaces and healthcare workers or patients or between healthcare workers and patients.[6−13] Surfaces act as a reservoir for contamination and involve door handles, keyboards, taps, sterile packaging, telephones, bed rails, mops, walls, ward fabric/plastics, medical equipment, counters, bedside tables, sheets, surgical trays, and stethoscopes.[6−13]

Improvements in medicine and surgery rely on a wide range of medical devices of which the catheter is the most commonly used.[14] Catheters are medical devices used in the transfer of fluids from and to the body in addition to drug administration. Flexible polymeric materials (e.g., polyurethane and silicone) are used to manufacture catheters. The surface properties of catheters are frequently rough and nonshedding meaning that they can be easily colonized by bacteria.[14,15] There is a growing body of literature that recognizes the importance of medical device-related infections in causing significant morbidity especially in the case of implanted synthetic medical devices.[16−18] Among medical devices, catheter-related infections are a cause of a high proportion of HAI. Intravascular and urinary catheters are two of the most common sources of hospital bloodstream infections, which are due to their prevalent use in medical care.[19] The three most common sources of catheter failure and dysfunction are formation of a biofilm that causes the development of thrombus formation, a fibrin sheath, and infection.[20] An antimicrobial catheter surface would considerably decrease the infections.[21]

Incorporation of photosensitizer dyes, including crystal violet (CV), methylene blue (MB), and toluidine blue O, into a polymer provides a method to develop photoactivatable bactericidal surfaces.[22−24] Photosensitive dyes have been encapsulated into polymeric materials using a simple "swell−encapsulation−shrink" method and displayed antimicrobial activity against a variety of bacteria. The swell−encapsulation−shrink approach involves immersing the polymer in an

Received: March 22, 2018
Accepted: May 21, 2018
Published: June 22, 2018

DOI: 10.1021/acsomega.8b00552
ACS Omega 2018, 3, 6779−6786

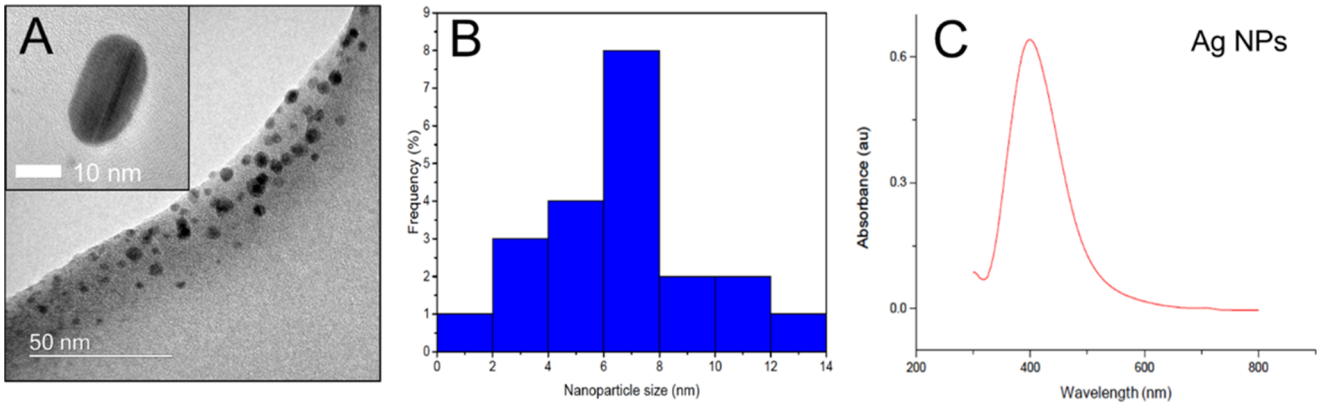

Figure 1. Ag NPs (A) HR-TEM image, (B) nanoparticle size distribution, and (C) absorption spectra of Ag NP solution.

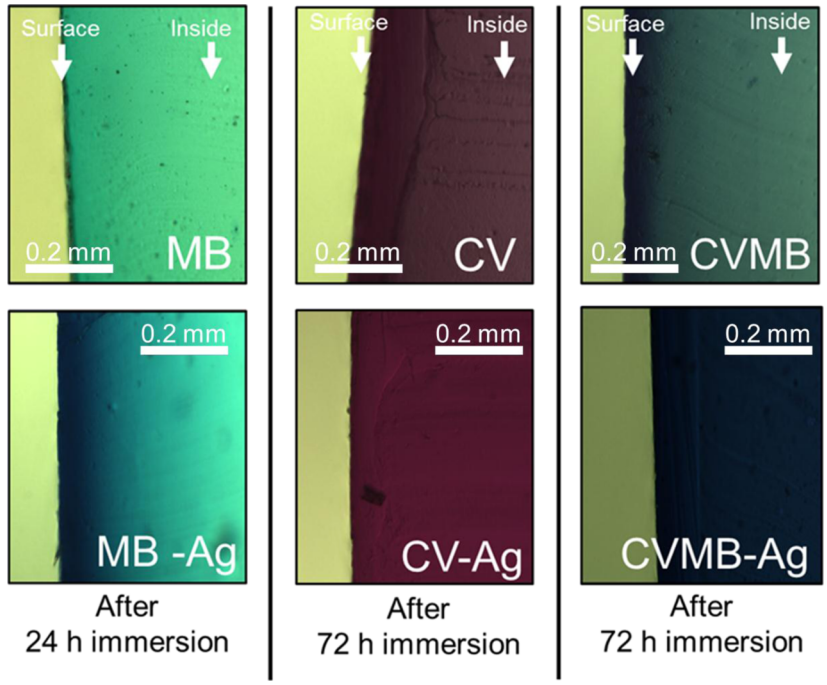

Figure 2. Distribution of dye in silicone after swell-encapsulation-shrink process for 24 or 72 h in silicone.

organic solution of the photosensitizer that enables swelling of the silicone polymer and allows the diffusion of the dye molecules uniformly within the polymeric matrix. The polymer is subsequently removed from the solution, the solvent evaporates with shrinkage of the polymer to its original size leaving the photosensitizer dye encapsulated in the polymer.[25] Photoactivated antimicrobials have the advantage such that it is unlikely that bacterial resistance will develop to them because the bactericidal properties occur through multiple pathways.[26,27] Light-activated antimicrobial agents, including molecular dyes, can destroy bacterial cells when they are illuminated with light by generating reactive oxygen species (ROS) and/or singlet oxygen. Despite the fact that the photosensitive dyes are not toxic, during illumination with visible light, the molecule is stimulated from ground singlet state to an excited triplet state, creating cytotoxic ROS through photochemical reaction type I and/or type II: through type I, the dye in the triplet state interacts with the surrounding environment, resulting in production of ROS, and through type II, the molecular energy in a triplet state is transferred to triplet oxygen ($^3O_2$) and then it produces singlet oxygen ($^1O_2$).[28,29]

Different kinds of metallic nanomaterials, such as copper, zinc, titanium, magnesium, gold, and silver, have been comprehensively studied with regard to their toxicity and bactericidal properties. So far, silver nanoparticles (Ag NPs) have demonstrated the most effective bactericidal activity against microorganism.[22,30] Ag NPs are used in a range of applications, e.g., burn treatment, dental materials, coating stainless steel materials, textile fabrics, and water treatment. Additionally, Ag NPs showed low volatility, high thermal stability, and low toxicity for human cells.[22,30,31]

In this study, we combine CV and MB into silicones together with Ag NPs by the swell−encapsulation−shrink process and the materials were tested for antimicrobial activity under white light and dark conditions. Optical microscopy and X-ray photoelectron spectroscopy (XPS) showed that the dyes and Ag NPs are well encapsulated into the silicone, and leaching tests confirmed that the materials are stable in water over a long period of time. In antimicrobial tests, the materials showed very potent bactericidal activity under white light and also showed antimicrobial activity in the dark. This is the first time that two

DOI: 10.1021/acsomega.8b00552
ACS Omega 2018, 3, 6779−6786

photosensitizer dyes have been used in combination with Ag NPs.

RESULTS AND DISCUSSION

Silver nanoparticles (NPs) were synthesized by mixing and heating aqueous solutions of sodium borohydride and trisodium citrate (TSC), followed by the dropwise addition of silver nitrate to the heated mixture of reductants. The solution was further heated until the formation of a bright yellow color. As shown in Figure 1A, high-resolution transmission electron microscopy (HR-TEM) analysis showed that the nanoparticles are spherical and polydispersed and the average nanoparticle size of Ag NPs was 6.8 ± 4.5 nm in diameter (Figure 1B). Energy-dispersive spectrometry analysis confirmed the existence of Ag NPs without impurities. The absorption spectra of Ag NPs solution showed a peak at 398 nm (Figure 1C), and the concentration of Ag in the particle solution was about 36 ppm.

A facile swell−encapsulation−shrink method was used to encapsulate Ag NPs into medical-grade silicone. CV/MB/Ag NPs encapsulated into silicones were prepared using a two-step dipping process. Silicone samples (10 mm × 10 mm × 1 mm) with various dipping times were analyzed using optical microscopy. The thinly sliced silicone side sections were imaged using charge-coupled device camera to confirm dye diffusion into the inside of the silicone. At the beginning, absorption was predominately near to the silicone surface and with increasing exposure time, the dye absorbed throughout the silicone (Figure S1). As shown in Figure 2, the coloration of samples is dark blue for silicone-incorporating Ag NPs and MB, dark purple for silicone-containing Ag NPs and CV, and dark blue-purple for silicone-incorporating MB, CV, and Ag NPs. Ag NP-encapsulated silicone had a more intense color than silicone without Ag NPs, indicating that the addition of Ag NPs enables enhanced dye uptake into the silicone. As a result, the main absorbance spectra of the NP-encapsulated samples were higher than the sample without the NPs.

As shown in Figure 3, UV−vis absorbance spectroscopy measurements of silicone samples incorporating Ag NPs and dye showed greater absorbance signals compared to those only incorporating Ag NPs or dyes. The silicone-incorporating MB or CV absorbed intensely with maxima at 650 and 590 nm, respectively. The silicone encapsulated with the two dyes and the Ag NPs demonstrated absorption peaks at 650 and 600 nm, corresponding to MB and CV, respectively. The presence of Ag nanoparticles (vide infra from XPS) in the silicone increased the dye peak intensity, whereas the peak shape and position stayed the same compared to silicone-incorporating dyes alone. However, the combination of Ag NPs, CV, and MB displayed a small shift in the peak maxima position from 590 to 600 nm. It might be because Ag NPs had an interaction with the dyes.[32] Additionally, as shown in Figure S2, the characteristic UV−vis signal of the nanoparticles was not observed when Ag NPs only were embedded into silicone. It was considered that the number of Ag NPs inside the polymer was not enough to be easily detected by the spectrometer or that the signal of Ag NPs was covered by the absorbance spectrum of the polymer because allowing for polymer thickness absorbance at 389 nm was higher than that of Ag NPs suspension for encapsulation.

X-ray photoelectron spectroscopy (XPS) was used to analyze the existence of Ag NPs on the polymer surface and within the polymer bulk for Ag NP-encapsulated silicone samples. As shown in Figure 4, XPS analysis of the Ag NP-encapsulated

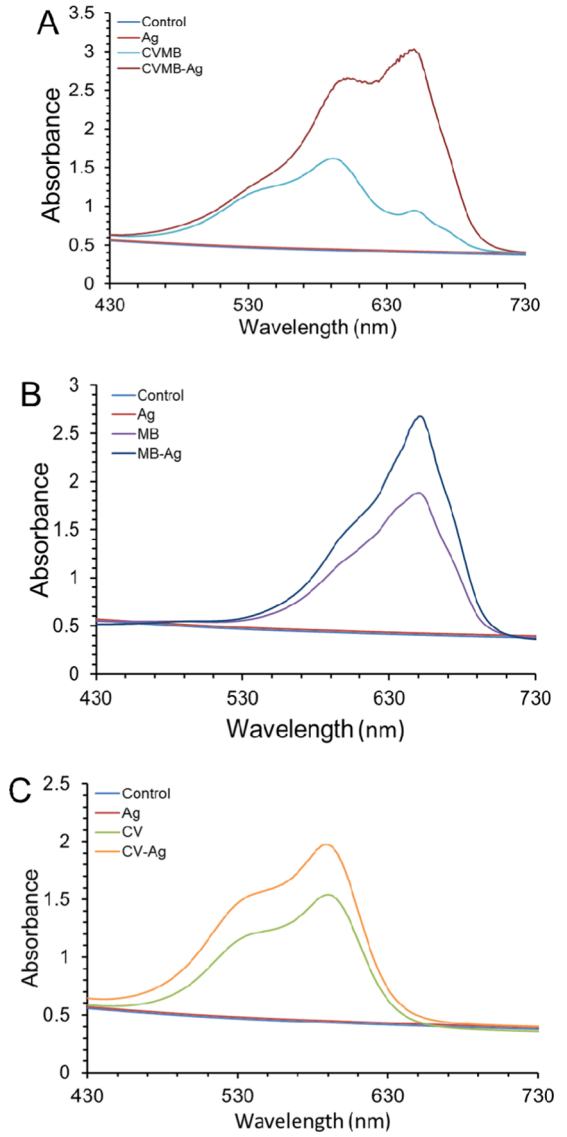

Figure 3. Absorbance spectra of (a) CVMB, CVMB-Ag; (b) MB, MB-Ag; and (c) CV, CV-Ag NPs.

silicone sample showed an indication of silver, identifying the existence of Ag NPs embedded both within the polymer matrix and at the polymer surface. As shown in the figure, XPS shows evidence of Ag NPs at the sample surfaces and within the polymer bulk. A doublet peak in the Ag (3d) region corresponds to silver $3d^{5/2}$ and $3d^{3/2}$ that consist of two peaks 368.3 and 373.3 eV binding energies, respectively, showing evidence of Ag on the surface and within the silicone bulk. XPS depth profile data results indicate the presence of Ag NPs encapsulated on the surface and within the polymer matrix. To investigate the concentration of Ag NPs encapsulated into the polymer, the UV−vis spectra of Ag NPs suspension were measured before and after encapsulation. The silicone sample was placed into Ag NPs suspension for 24 h. Ag (1.5 ppm) in the suspension was encapsulated into the polymer after 24 h indicating that 41% of Ag NPs was encapsulated.

In previous research, it was reported that swell−encapsulation−shrink process decreased significantly the water contact angle of polyurethane resulting in a change from hydrophobic and hydrophilic.[24] However, as shown in Table 1, when the

DOI: 10.1021/acsomega.8b00552
ACS Omega 2018, 3, 6779−6786

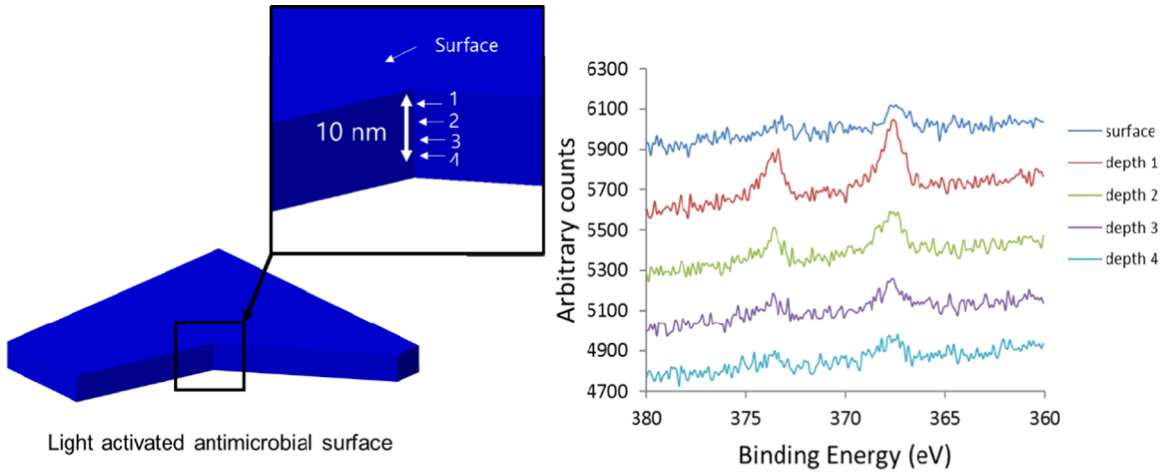

Figure 4. X-ray photoelectron spectra of silver/silicone in different regions of the polymer.

Table 1. Average Static Water Contact Angle Measurements (deg) ± Standard Deviation of Untreated and Treated Silicone Samples

sample	water contact angle (deg)	sample	water contact angle (deg)
untreated	116.1 ± 2.5	CVMB	117.2 ± 3.4
control	116.9 ± 2.3	CV-Ag	117.6 ± 2.8
CV	115.9 ± 3.3	MB-Ag	118.2 ± 2.7
MB	117.9 ± 2.5	CVMB-Ag	120 ± 1.8
Ag	117 ± 2.1		

nanoparticles and dyes were encapsulated into silicone, the change in water contact angle of silicone was minor, indicating that the process does not affect its hydrophobicity.

The extent to which CV and MB were released from the silicone-incorporating dyes was measured using a UV−vis spectrometer. The treated samples with dye were immersed in phosphate-buffered saline (PBS) solution up to a period of 216 h. Figure S3 shows the concentrations of MB and CV dyes released from the treated sample. The total concentration of the dye leached from silicone was below 0.02 ppm over a period of 200 h. The results confirmed that the leakage of CV and MB into the surrounding PBS solution is negligible.

The bactericidal activities of treated and control samples were examined against *Escherichia coli*, Gram-negative bacterium, and *Staphylococcus aureus*, Gram-positive bacterium. The visible light source that was used to initiate bactericidal activity was less intense than most of those used in U.K. hospital environments (3000 lx).[26,33] The light-activated bactericidal activities of the following samples were determined: solvent-treated silicone (control), MB- or CV-only encapsulated silicone (MB or CV), Ag NP-only encapsulated silicone (Ag), Ag NPs and MB encapsulated into silicone (MB-Ag), Ag NP- and CV-encapsulated silicone (CV-Ag), MB- and CV-encapsulated silicone without Ag NPs (CVMB), and MB- and CV-encapsulated silicone with Ag NPs (CVMB-Ag).

The capacity of the materials to cause photoactivatable killing of bacteria was determined using a white light source with an average light intensity of 970 ± 80 lx. The light intensity distribution ranged from high to low between 800 and 1100 lx from the center toward the edge (Figure S4). As shown in Figure 5A, Ag MB, MB-Ag, and CV demonstrated no significant kill of *S. aureus* by comparison with the control silicone sample in dark conditions after incubation for 3 h. However, CV-Ag, CVMB, and CVMB-Ag silicone samples caused a statistically significant (p value <0.05 compared to the control) reduction in the number of *S. aureus* compared to that of the control silicone sample in the dark for the same period of time; 0.47 log, 0.32 log, and 0.35 log kills were on CV-Ag, CVMB, and CVMB-Ag samples, respectively. After 3 h incubation in white light, photosensitizer dye-encapsulated samples showed photoactivated bactericidal activity. Among them, MB-Ag, CV-Ag, CVMB, and CVMB-Ag samples showed potent photobactericidal activity. The MB-Ag, CV-Ag, and CVMB samples had 0.74 log, 0.61 log, and 0.47 log kills (p value <0.05 compared to the control). The CVMB-Ag sample demonstrated the most lethal photosensitization, with the number of bacteria reduced below the detection limit within 3 h of incubation (>2.55 log reduction and p value <0.01 compared to the control).

As shown in Figure 5B, the antimicrobial activity of the light-activated bactericidal surfaces was observed against *E. coli* after 5 h incubation time. Compared with the control, the CV-Ag and CVMB-Ag samples showed statistically significant reduction in the number of bacteria (p value <0.01 compared to the control) after 5 h incubation in the dark, whereas the antimicrobial activity of Ag, MB, CV, MB-Ag, and CVMB sample was negligible. The CV-Ag and CVMB-Ag silicone samples showed strong bactericidal activities with 0.48 log and 2.1 log reductions in the dark, respectively (p value <0.01 compared to the control). Upon 5 h exposure of white light, MB-Ag, CV, CV-Ag, CVMB, and CVMB-Ag samples showed an enhanced bactericidal activity (p value <0.01 compared to the control). The MB-Ag- and CV-only encapsulated samples demonstrated 0.44 log and 0.73 log kills upon 5 h white light illumination, and the CV-Ag and CVMB samples also showed an enhanced activity with 1.6 log and 1.21 log reductions, respectively. The dual-dye-encapsulated sample with silver nanoparticles (CVMB-Ag) showed the most potent bactericidal activity upon 5 h of white light illumination with bacterial numbers reduction below the detection limit (>3 log and p value <0.01 compared to the control).

This study shows that potent lethal photoactivated silicone has the capacity to cause killing of *S. aureus*, after shorter illumination time than *E. coli*. The results from our work have shown that the inactivation of bacteria is associated with the type of bacterium. The susceptibility of *E. coli*, Gram-negative bacterium, is less than *S. aureus*, Gram-positive bacterium,

DOI: 10.1021/acsomega.8b00552
ACS Omega 2018, 3, 6779−6786

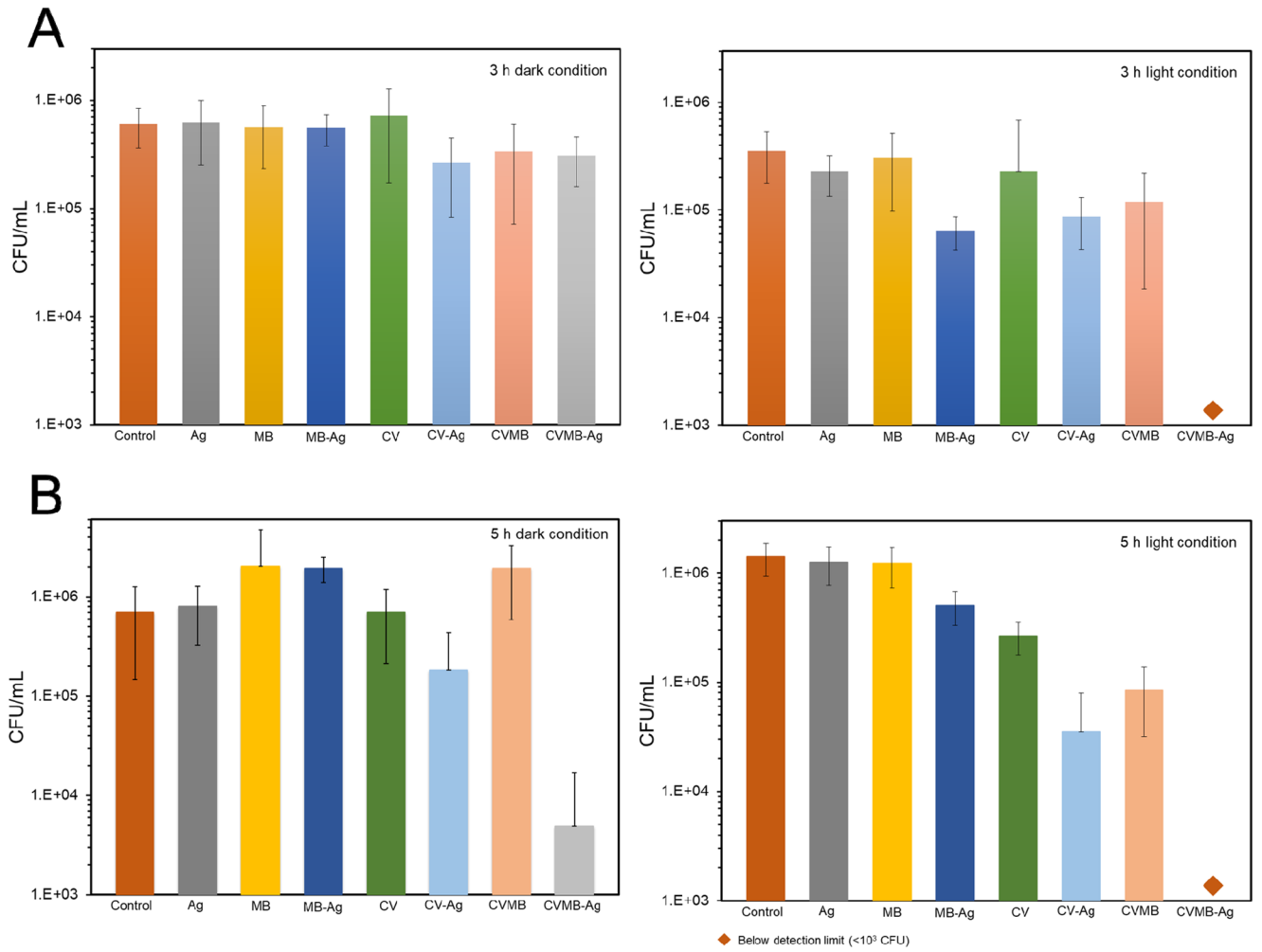

Figure 5. Antimicrobial activity of treated silicone samples on (A) *S. aureus* and (B) *E. coli* under dark condition and white light conditions. In all tests, the temperature was maintained at a constant 20 °C.

relating to different cell walls that respond differently to the radical threat.[34]

It is known that Ag NPs, crystal violet, and methylene blue have intrinsic bactericidal activity. Ag ions or the dyes themselves dissociated from the substances cause bacterial death.[35,36] However, after encapsulation, each of them did not represent any bactericidal activity in the dark, thus indicating that the cytotoxic effect of Ag or the dyes was not sufficient to reduce bacterial viability. The combination of Ag NPs and crystal violet or crystal violet and methylene blue in the polymer produced a reduction in the number of viable bacteria in dark. This might be because of multitype ion attack produced from silver and the dyes. This trend was in agreement with previous research.[24] Additionally, MB-Ag sample did not show an enhanced bactericidal activity in dark and this is mainly due to methylene blue, which has a weak bactericidal activity compared to crystal violet.[37]

On exposure to the white light, crystal violet or methylene blue molecules are promoted from a ground state to an excited single state and then they transform to a triplet state via intercrossing system or they return to a ground state through energy loss depending on surrounding or dye molecules conditions.[28,29] The molecules in a triplet state undergo two different pathways including photoreaction types I and II. In photoreaction type I, they produce reactive oxygen species (ROS) through an interaction with their environment, and in the reaction II, the energy is transferred to triplet oxygen species resulting in single oxygen ($^1O_2$) generation. Bacteria in the vicinity of the sample surface are killed by multisite attack of the generated ROS and $^1O_2$.[28,29] In previous studies, it was reported that Au or Ag nanoparticle addition into the dyes did not increase $^1O_2$ generation under white light condition, indicating that photoreaction type II is not enhanced by the particles.[24,38] Thus, it is speculated that the addition of silver nanoparticles into dye-impregnated silicone enhances photoreaction type I, resulting in an enhanced photobactericidal activity with an increase of ROS generation

Although MB is distributed comparatively uniformly throughout the polymer, CV-encapsulated polymer exhibits high concentrations in a layer on the polymer surface, as analyzed using optical microscopy. This mechanism can clarify the difference between MB- and CV-encapsulated silicones because the dye on the surface would cause enhanced generation of ROS that results in exceptional kill of surface-located bacteria.

The ROS diffusion distance generated during photosensitization of a dye is probably between 10 and 100 nm within the polymer, and the half-life time of ROS is less than 1 μs in physiological environment.[39] Because of this short diffusion distance of ROS within a polymer, the photosensitizer

DOI: 10.1021/acsomega.8b00552
ACS Omega 2018, 3, 6779−6786

encapsulated within the polymer bulk is redundant in terms of bactericidal activity. Thus, the photobactericidal activity was mainly induced by the dyes near to the sample surface.

To validate the bactericidal efficacy of the Ag NP-encapsulated surface, photobactericidal activity was compared to results in previous studies.[33,40,41] The study of Ag NP-coated titania thin film showed that Ag NPs could enhance photobactericidal effect against *E. coli* under a white light intensity of 5000 lx.[33] The combination of Ag NPs, CV, and MB dyes produced stronger photobactericidal activities against *E. coli* and *S. aureus* than those of Ag NPs and titania because with a white light intensity of average 970 lx, our combination reduced bacterial viability to below detection limit within 3 h (*S. aureus*) or 5 h (*E. coli*). Compared to multidyed photobactericidal surface[40] and zinc oxide NP-encapsulated polymer,[41] Ag NP-encapsulated surface dropped the required light intensity to obtain bacterial kill by a quarter.

The bactericidal activity of these novel dual dyes and silver-encapsulated surfaces would be the most effective in places that have higher light intensity, for instance, operating theaters and examination rooms.[34] It was shown in this study that although relatively low light intensity was used for short exposure times, exceptional bacteria kill can still be achieved. However, it should be considered that very high bacterial load ($\sim 1.3 \times 10^6$ CFU cm^{-2} for *E. coli* and $\sim 2.2 \times 10^6$ CFU cm^{-2} for *S. aureus*) was used to observe the efficiency of antimicrobial activity of the polymer in these experiments. In comparison to hospital surfaces, the contaminated surfaces reserve notably less than the level used in these experiments (up to an equivalent of 3060 CFU cm^{-2} with average values of <100 CFU cm^{-2}).[40]

In previous studies, the photostability test was performed under a white light lamp with a light intensity of 12 500 lx for 29 days, and it was shown that dual-dye- and Au nanoparticle-encapsulated polymer maintained its absorbance spectra over a long period of time.[40] The light intensity of the lamp used in this study was about 13 times lower than 12 500 lx. Thus, it is speculated that under our white light condition, the photobactericidal polymers will maintain their activity for far longer than 29 days and of the order of a year.

CONCLUSIONS

Through a swell−encapsulation−shrink process, methylene blue, crystal violet, and silver nanoparticles were encapsulated into medical-grade silicone that is in common use in healthcare environments. XPS and optical microscopy demonstrated that the dyes and silver nanoparticles were successfully penetrated inside the polymer, and UV−vis spectroscopy showed that the addition of silver nanoparticles enhanced the absorbance features of either dyes crystal violet and methylene blue. In leaching test, the dyes in the polymer were shown to be stable over a period of 210 h with minor leaching into the surrounding liquid. Bactericidal test showed that when silver nanoparticles and dual-dye-encapsulated samples were exposed to white light, their bactericidal activity was significantly enhanced, achieving >3 log reduction of viable bacteria after several hours exposure of white light (3 h for *S. aureus* and 5 h for *E. coli*). It is expected that the photobactericidal surfaces that we developed is useful to reduce surface contamination by bacteria and thus the nosocomial infection in hospital facilities.

EXPERIMENTAL SECTION

Chemical and Reagents. $AgNO_3$ (silver nitrate), $Na_3C_6H_5O_7 \cdot 2H_2O$ (sodium citrate tribasic dehydrate), and acetone were purchased from Sigma-Aldrich Chemical Co. Sodium borohyride ($NaBH_4$) was purchased from BDH Chemicals Ltd. Medical-grade flat silicone sheets (thickness 1.0 mm) were purchased from NuSil (Polymer Systems Technology, Ltd.). Deionized (DI) water (resistivity 15 MΩ cm) was used during the experiments.

Synthesis of Silver Nanoparticles. Silver nanoparticles were prepared using sodium borohydride ($NaBH_4$) and trisodium citrate (TSC),[42] as primary and secondary reductants, respectively, in addition to a stabilizing agent. The reduction processes were performed at 60 and 90 °C and provided mainly through sodium borohydride and trisodium citrate, respectively. A usual preparation is as follows: the required volumes of freshly prepared aqueous solutions of $NaBH_4$ (2×10^{-3} M) and TSC (4.25×10^{-3} M) were mixed and heated to 60 °C under vigorous stirring for 30 min to make a homogenous solution. After 30 min, 4 mL of $AgNO_3$ solution (1×10^{-3} M) was added dropwise to the mixture solution and then the temperature was further raised to 90 °C. The temperature was maintained at 90 °C for 20 min until a bright yellow color was obtained. The nanoparticle suspension was then allowed to cool to room temperature.

Preparation of Visible Light-Activated Antimicrobial Polymers. Preparation of MB only and MB with Ag NPs samples: as shown in Figure S5A,D, methylene blue (MB) solutions were prepared at a concentration of 700 ppm in a mixture of acetone (9 mL) and DI water (1 mL) or NPs (1 mL). Silicone samples (10 mm × 10 mm × 1 mm) were immersed in 10 mL of the solutions and kept in the dark for 24 h. The silicone samples were collected from the solutions and washed two times using DI water and then air-dried for 24 h in the dark at room temperature.

Preparation of CV-only samples: as shown in Figure S5B, crystal violet (CV) solutions were prepared at a concentration of 1000 ppm in DI water. Silicone samples were placed in 10 mL of the solutions and kept in the dark for 72 h, the samples were then collected from the solution, washed two times using DI water, and then air-dried for 24 h in the dark at room temperature.

Preparation of Ag NP-encapsulated samples: as shown in Figure S5C, the samples were placed in a mixture of acetone (9 mL) and Ag NPs (1 mL) for 24 h, then collected from the solution, washed two times using DI water, and air-dried for 24 h in the dark at room temperature.

Preparation of CV samples with Ag NPs: as shown in Figure S5F, the samples were immersed in a mixture of acetone (9 mL) and Ag NPs (1 mL) for 24 h and then immersed in CV solutions for 72 h. The samples were collected from the solution, washed two times by DI water, and then air-dried for 24 h in the dark at room temperature.

Preparation of CVMB samples: as shown in Figure S5E, the samples were immersed in MB solutions for 24 h and then placed in CV solution for 72 h. The samples were collected from the solution, washed two times using DI water, and then air-dried for 24 h in the dark at room temperature.

Preparation of CVMB samples with Ag NPs: as shown in Figure S5G, the samples were immersed in the mixture of Ag NPs and MB for 24 h and then placed in CV solution for 72 h. They were collected from the solution, washed two times using

DOI: 10.1021/acsomega.8b00552
ACS Omega 2018, 3, 6779−6786

DI water, and then air-dried for 24 h in the dark at room temperature.

Materials Characterization. Ag NPs suspension was drop-casted onto a 300 Cu mesh lacey carbon film grid (Agar Scientific Ltd.) and then air-dried for 1 h. The images of nanoparticles were taken by a JEOL 2100 high-resolution transmission electron microscope equipped with an energy-dispersive X-ray. The imageJ was used to analyze TEM images.

The UV−vis absorption spectra of Ag NPs suspensions, control, and treated silicone samples were measured by a UV−vis spectrometer Lamb 25 (PerkinElmer Inc., Winter St., CT). Absorption was measured from 400 to 800 nm for treated silicone samples and 300−800 nm wavelength for Ag NPs solution.

X-ray photoelectron spectroscopy (XPS) was performed by a Thermo K-Alpha spectrometer to determine silver as a function of polymer depth. All binding energies were calibrated to the C 1s peak at 284.5 eV.

FTA 1000 drop shape instrument was used to determine the difference in surface hydrophobicity before and after the treatment on the silicone, and the water contact angle (∼5.0 μL) was analyzed by the FTA32 software.[43]

The stability of the dye-encapsulated silicone was tested in phosphate-buffered saline (PBS) at room temperature. All treated samples encapsulated with dye were immersed in PBS for an extended period of time. The UV−vis spectra of absorbance of PBS solution were measured periodically (596 nm, Pharmacia Biotech Ultrospec 2000) to determine leaching amount of the dye from the treated silicone into the surrounding solution. The concentration of MB and CV that was released into the PBS solution was examined by comparison of the absorbance of PBS at 665 and 584 nm with a MB and CV calibration curve.

Uptake of Ag NPs into Silicone. To investigate the concentration of Ag NPs encapsulated into silicone, the silicone was placed in a mixture of acetone (9 mL) and Ag NPs (1 mL) for 24 h. The UV−vis absorbance spectra of Au NPs suspension were measured before and after the encapsulation. Through the change of absorption at 398 nm, the concentration of Ag NPs inside silicone can be determined.

The amount of the NPs encapsulated into the polymer was calculated as follows

$$\text{Au conc. in the polymer (ppm)} = 3.6\ \text{ppm} \times \left(1 - \frac{\text{AU}_{\text{before}} - \text{AU}_{\text{after}}}{\text{AU}_{\text{before}}}\right) \quad (1)$$

where $\text{AU}_{\text{before}}$ indicates the absorption of NP suspension before the encapsulation and AU_{after} represents the absorption of NPs suspension after the treatment; 3.6 ppm indicates Ag concentration in the suspension.

Antimicrobial Test. The antimicrobial activities of the samples were tested against *E. coli* (strain ATCC 25922) and *S. aureus* 8324-5, both of which were stored at −70 °C in brain-heart-infusion (BHI) broth (Oxoid Ltd., Hampshire, England, U.K.) containing 20% (v/v) glycerol and propagated on either MacConkey agar or mannitol salt agar (Oxoid Ltd., Hampshire, England, U.K.) for *E. coli* and *S. aureus*, respectively. BHI broth (10 mL) was inoculated with one bacterial colony and cultured at 37 °C for 18 h with a shaking of 200 rpm. After 18 h, the bacteria were harvested through centrifugation (20 °C, 3000*g*, 15 min), washed using 10 mL of PBS two times, and then 1000-fold diluted to obtain bacterial suspension with 10^6 CFU mL^{-1}. Bacterial suspension (25 μL) was inoculated onto the surface of the treated silicone sample. The samples were placed into plastic Petri dishes containing moistened filter paper to maintain humidity and exposed to a white light intensity of 970 lx, while an identical set of samples was maintained in the dark. After light exposure, the modified sample was placed into 5 mL of PBS and vortexed for 1 min to wash out bacteria from the sample to PBS. The bacterial suspension was serially diluted, plated onto MacConkey agar or mannitol salt agar, and cultured at 37 °C for 24 h (*E. coli*) and 48 h (*S. aureus*), respectively. The colonies that were grown on the plates were counted.

Statistical Analysis. Statistic *t* test of the results was performed using Excel (Microsoft Corporation).

■ ASSOCIATED CONTENT

Supporting Information

The Supporting Information is available free of charge on the ACS Publications website at DOI: 10.1021/acsomega.8b00552.

Cross-sectional image of treated polymers (Figure S1), UV−vis spectra of control and silicone with Ag NPs (Figure S2), leaching of MB and CV from silicone polymer (Figure S3), intensity distribution of white light used for illumination (Figure S4), and preparation of antimicrobial samples (Figure S5) (PDF)

■ AUTHOR INFORMATION

Corresponding Author

*E-mail: i.p.parkin@ucl.ac.uk. Tel: 44(0)207 679 4669.

ORCID

Gi Byoung Hwang: 0000-0003-0874-8390

Notes

The authors declare no competing financial interest.

■ ACKNOWLEDGMENTS

The authors would like to thank Dr. Kristopher Page (Chemistry Department, UCL) for his advice.

■ REFERENCES

(1) House of Commons Committee of Public Account. *Improving Patient Care by Reducing the Risks of Hospital Acquired Infection: A Progress Report*, 2004/05.

(2) House of Commons Committee of Public Account. *Reducing Healthcare Associated Infection in Hospitals in England*, 2009.

(3) Office for National Statistics. Deaths involving Clostridium : England and Wales 2003−07. *Health Stat. Q.* **2008**, *39*, 67.

(4) Office for National Statistics. Deaths involving MRSA: England and Wales. *Health Stat. Q.* **2008**, *39*, 56.

(5) Centers for Disease Control and Prevention (CDC). *National and State Healthcare Associated Infections Progress Report*, 2015.

(6) Oie, S.; Hosokawa, I.; Kamiya, A. Contamination of room door handles by methicillin-sensitive/methicillin-resistant *Staphylococcus aureus*. *J. Hosp. Infect.* **2002**, *51*, 140.

(7) Dietze, B.; Rath, A.; Wendt, C.; Martiny, H. Survival of MRSA on sterile goods packaging. *J. Hosp. Infect.* **2001**, *49*, 255.

(8) Oie, S.; Kamiya, A. Survival of methicillin-resistant *Staphylococcus aureus* (MRSA) on naturally contaminated dry mops. *J. Hosp. Infect.* **1996**, *34*, 145.

(9) Neely, A. N.; Maley, M. P. Survival of *Enterococci* and *Staphylococci* on hospital fabrics and plastic. *J. Clin. Microbiol.* **2000**, *38*, 724.

(10) Bures, S.; Fishbain, J. T.; Uyehara, C. F.; Parker, J. M.; Berg, B. W. Computer keyboards and faucet handles as reservoirs of

DOI: 10.1021/acsomega.8b00552
ACS Omega 2018, 3, 6779−6786

nosocomial pathogens in the intensive care unit. *Am. J. Infect. Control* **2000**, *28*, 465.
(11) Cohen, H. A.; Amir, J.; Matalon, A.; Mayan, R.; Beni, S.; Barzilai, A. Stethoscopes and otoscopes—a potential vector of infection? *Fam. Pract.* **1997**, *14*, 446.
(12) Panagea, S.; Chadwick, P. R. *J. Clin. Pathol.* **1996**, *49*, 687.
(13) Dalstrom, D. J.; Venkatarayappa, I.; Manternach, A. L.; Palcic, M. S.; Heyse, B. A.; Prayson, M. J. Heat tolerance of vancomycin resistant *Enterococcus faecium*. *J. Bone Jt. Surg., Am. Vol.* **2008**, *90*, 1022.
(14) Trautner, B. W.; Darouiche, R. O. Catheter-associated infections: pathogenesis affects prevention. *Arch. Intern. Med.* **2004**, *164*, 842.
(15) Wilson, M. *Mcrobial Inhabitants of Humans: Their Ecology and Role in Health and Disease*, 1st ed.; Cambridge University Press: Cambridge, 2005.
(16) Hellmann, M.; Mehta, S. D.; Bishai, D. M.; Mears, S. C.; Zenilman, J. M. The estimated magnitude and direct hospital costs of prosthetic joint infections in the United States, 1997 to 2004. *J. Arthroplasty* **2010**, *25*, 766.e1.
(17) Sampedro, M. F.; Patel, R. Infections associated with long-term prosthetic devices. *Infect. Dis. Clin North Am.* **2007**, *21*, 785.
(18) Tokarczyk, A. J.; Greenberg, S. B.; Vender, J. S. Death, dollars, and diligence: prevention of catheter-related bloodstream infections must persist! *Crit. Care Med.* **2009**, *37*, 2320.
(19) Noimark, S.; Dunnill, C. W.; Wilson, M.; Parkin, I. P. The role of surfaces in catheter-associated infections. *Chem. Soc. Rev.* **2009**, *38*, 3435.
(20) Dwyer, A. Surface-treated catheters—a review. *Semin. Dial.* **2008**, *21*, 542.
(21) Furno, F.; Morley, K. S.; Wong, B.; Sharp, B. L.; Arnold, P. L.; Howdle, S. M.; Bayston, R.; Brown, P. D.; Winship, P. D.; Reid, H. J. Silver nanoparticles and polymeric medical devices: a new approach to prevention of infection? *J. Antimicrob. Chemother.* **2004**, *54*, 1019.
(22) Sehmi, S. K.; Noimark, S.; Bear, J. C.; Peveler, W. J.; Bovis, M.; Allan, E.; MacRobert, A. J.; Parkin, I. P. Lethal photosensitisation of *Staphylococcus aureus* and *Escherichia coli* using crystal violet and zinc oxide-encapsulated polyurethane. *J. Mater. Chem. B* **2015**, *3*, 6490.
(23) Hwang, G. B.; Allan, E.; Parkin, I. P. White light-activated antimicrobial paint using crystal violet. *ACS Appl. Mater. Interfaces* **2016**, *8*, 15033.
(24) Hwang, G. B.; Noimark, S.; Page, K.; Sehmi, S.; Macrobert, A. J.; Allan, E.; Parkin, I. P. White light-activated antimicrobial surfaces: effect of nanoparticles type on activity. *J. Mater. Chem. B* **2016**, *4*, 2199.
(25) Ozkan, E.; Allan, E.; Parkin, I. P. The antibacterial properties of light-activated polydimethylsiloxane containing crystal violet. *RSC Adv.* **2014**, *4*, 51711.
(26) Decraene, V.; Pratten, J.; Wilson, M. An assessment of the activity of a novel light-activated antimicrobial coating in a clinical environment. *Infect. Control Hosp. Epidemiol.* **2008**, *29*, 1181.
(27) Wilson, M.; Pratten, J. Lethal photosensitisation of *Staphylococcus aureus* in vitro: effect of growth phase, serum, and pre-irradiation time. *Lasers Surg. Med.* **1995**, *16*, 272.
(28) Edmiston, C. E., Jr.; Daoud, F. C.; Leaper, D. Is there an evidence-based argument for embracing an antimicrobial (triclosan)-coated suture technology to reduce the risk for surgical-site infections?: A meta-analysis. *Surgery* **2013**, *154*, 89.
(29) Hamblin, M. R.; Hasan, T. Photodynamic therapy: a new antimicrobial approach to infectious disease? *Photochem. Photobiol. Sci.* **2004**, *3*, 436.
(30) Rai, M.; Yadav, A.; Gade, A. Silver nanoparticles as a new generation of antimicrobials. *Biotechnol. Adv.* **2009**, *27*, 76.
(31) Durán, N.; Marcato, P. D.; De Souza, G. I.; Alves, H. O.; Esposito, L. E. Antibacterial effect of silver nanoparticles produced by fungal process on textile fabrics and their effluent treatment. *J. Biomed. Nanotechnol.* **2007**, *3*, 203.
(32) Ji, J. H.; Bae, G. N.; Yun, S. H.; Jung, J. H.; Noh, H. S.; Kim, S. S. Evaluation of a silver nanoparticle generator using a small ceramic heater for inactivation of *S. epidermidis* bioaerosols. *Aerosol Sci. Technol.* **2007**, *41*, 786.
(33) Dunnill, C. W.; Page, K.; Aiken, Z. A.; Noimark, S.; Hyett, G.; Kafizas, A.; Pratten, J.; Wilson, M.; Parkin, I. P. Nanoparticulate silver coated-titania thin films—Photo-oxidative destruction of stearic acid under different light sources and antimicrobial effects under hospital lighting conditions. *J. Photochem. Photobiol., A* **2011**, *220*, 113.
(34) Decraene, V.; Pratten, J.; Wilson, M. Cellulose acetate containing toluidine blue and rose bengal is an effective antimicrobial coating when exposed to white light. *Appl. Environ. Microbiol.* **2006**, *72*, 4436.
(35) Docampo, R.; Moreno, S. N. The metabolism and mode of action of gentian violet. *Drug Metab. Rev.* **1990**, *22*, 161−78.
(36) Feng, Q. L.; Wu, J.; Chen, G. Q.; Cui, F. Z.; Kim, T. N.; Kim, J. O. A mechanistic study of the antibacterial effect of silver ions *on Escherichia coli* and *Staphylococcus aureus*. *J. Biomed. Mater. Res.* **2008**, *52*, 662−668.
(37) Wainwright, M.; Crossley, K. B. Methylene blue - a therapeutic dye for all seasons? *J. Chemother.* **2002**, *14*, 431−443.
(38) Perni, S.; Prokopovich, P.; Piccirillo, C.; Pratten, J.; Parkin, I. P.; Wilson, M. Toluidine blue-containing polymers exhibit potent bactericidal activity when irradiated with red laser light. *J. Mater. Chem.* **2009**, *19*, 2715.
(39) Perni, S.; Piccirillo, C.; Pratten, J.; Prokopovich, P.; Chrzanowski, W.; Parkin, I. P.; Wilson, M. The antimicrobial properties of light-activated polymers containing methylene blue and gold nanoparticles. *Biomaterials* **2009**, *30*, 89.
(40) Noimark, S.; Allan, E.; Parkin, I. P. Light-activated antimicrobial surfaces with enhanced efficacy induced by a dark-activated mechanism. *Chem. Sci.* **2014**, *5*, 2216.
(41) Noimark, S.; Weiner, J.; Noor, N.; Allan, E.; Williams, C. K.; Shaffer, M. S. P.; Parkin, I. P. Dual-mechanism antimicrobial polymer-ZnO nanoparticle and crystal violet-encapsulated silicone. *Adv. Funct. Mater.* **2015**, *25*, 1367.
(42) Fayaz, A. M.; Balaji, K.; Girilal, M.; Yadav, R.; Kalaichelvan, P. T.; Venketesan, R. Biogenic synthesis of silver nanoparticles and their synergistic effect with antibiotics: a study against gram-positive and gram-negative bacteria. *Nanomedicine* **2010**, *6*, 103.
(43) Sehmi, S. K.; Noimark, S.; Weiner, J.; Allan, E.; MacRobert, A. J.; Parkin, I. P. Potent antibacterial activity of copper embedded into silione and polyurethane. *ACS Appl. Mater. Interfaces* **2015**, *7*, 22807.

DOI: 10.1021/acsomega.8b00552
ACS Omega 2018, 3, 6779−6786